

# Endothelial NADPH Oxidase as the Source of Oxidants in Lungs Exposed to Ischemia or High K<sup>+</sup>

Abu B. Al-Mehdi, Guochang Zhao, Chandra Dodia, Kasumi Tozawa, Karen Costa, Vladimir Muzykantov, Chris Ross, Frank Blecha, Mary Dinauer, Aron B. Fisher

**Abstract**—We have previously demonstrated the generation of reactive oxygen species (ROS) in cultured bovine pulmonary artery endothelial cells (BPAECs) and in isolated perfused rat lungs exposed to high K<sup>+</sup> and during global lung ischemia. The present study evaluates the NADPH oxidase pathway as a source of ROS in these models. ROS production, detected by oxidation of the fluorophore, dichlorodihydrofluorescein, increased 2.5-fold in BPAECs and 6-fold in rat or mouse lungs exposed to high (24 mmol/L) K<sup>+</sup>. ROS generation was markedly inhibited by diphenyliodonium, a flavoprotein inhibitor, and by the synthetic peptide PR-39, an inhibitor of NADPH oxidase assembly, whereas allopurinol had no effect. With ischemia (1 hour), ROS generation by rat and mouse lungs increased 7-fold; PR-39 showed concentration-dependent inhibition of ROS production, with 50% inhibition at 3 μmol/L PR-39. ROS production in lungs exposed to high K<sup>+</sup> or ischemia was essentially abolished in mice with a “knockout” of gp91<sup>phox</sup>, a membrane-localized cytochrome component of NADPH oxidase; increased ROS production by these lungs after anoxia/reoxygenation was similar to control. PR-39 also inhibited ischemia and the high K<sup>+</sup>-mediated increase in lung thiobarbituric acid reactive substance. Western blotting of BPAECs and immunocytochemistry of BPAECs and rat and mouse lungs showed the presence of p47<sup>phox</sup>, a cytoplasmic component of NADPH oxidase and the putative target for PR-39 inhibition. In situ fluorescence imaging in the intact lung demonstrated that the increased dichlorofluorescein fluorescence in these models of ROS generation was localized primarily to the pulmonary endothelium. These studies demonstrate that ROS production in lungs exposed to ischemia or high K<sup>+</sup> results from assembly and activation of a membrane-associated NADPH oxidase of the pulmonary endothelium. (*Circ Res.* 1998;83:730-737.)

**Key Words:** p47<sup>phox</sup> ■ gp91<sup>phox</sup> ■ bovine pulmonary artery endothelial cell ■ diphenyliodonium ■ PR-39

Using the isolated perfused rat lung model, we recently demonstrated the increased generation of reactive oxygen species (ROS) in the ischemic lung provided that lung oxygenation was maintained throughout ventilation.<sup>1,2</sup> We have dubbed this model “oxygenated ischemia” to differentiate it from anoxic ischemia produced by arterial obstruction in other organs or in the nonventilated lung. Oxygenated ischemia does not lead to the anoxia-mediated metabolic changes associated with ischemia in other organs. We also have developed a perfused-lung model of anoxia/reoxygenation produced by sequential lung ventilation for 1 hour each with N<sub>2</sub> and O<sub>2</sub> and demonstrated ROS generation during the reoxygenation phase.<sup>3</sup> Although both of these models result in ROS production, evidence from studies with inhibitors indicates that different metabolic pathways are predominantly responsible.<sup>3</sup> ROS generation with lung-oxygenated ischemia is inhibited by diphenyliodonium (DPI), a flavoprotein inhibitor, but is insensitive to the xanthine oxidase inhibitor allopurinol. The inverse was demonstrated with anoxia/

reoxygenation: ROS generation is insensitive to DPI but is inhibited by allopurinol.

Although decreased ATP generally is accepted as a triggering mechanism for ROS generation with anoxia/reoxygenation,<sup>4</sup> the mechanism with oxygenated ischemia must be different, since tissue oxygenation is preserved and lung ATP content remains at control levels.<sup>1,5</sup> To explain ROS generation with oxygenated ischemia, we investigated mechanisms other than anoxia-associated metabolic effects as a potential trigger. Using membrane potential sensitive dyes, we provided evidence that generation of ROS with decreased flow was associated with cell membrane depolarization.<sup>5</sup> To further explore the relationship between changes in lung membrane potential and ROS generation, we developed a depolarization model by perfusing isolated rat lungs or incubating bovine pulmonary artery endothelial cells (BPAECs) with high external K<sup>+</sup>.<sup>6,7</sup> High K<sup>+</sup> with either preparation resulted in increased ROS generation, providing support for the hypothesis that membrane depolarization can trigger ROS

Received March 25, 1998; accepted July 1, 1998.

From the Institute for Environmental Medicine (A.B.A.-M., G.Z., C.D., K.T., K.C., V.M., A.B.F.), University of Pennsylvania Medical Center, Philadelphia, Pa; the Department of Anatomy and Physiology (C.R., F.B.), Kansas State University College of Veterinary Medicine, Manhattan, Kan; and the Department of Pediatrics (M.D.), Indiana University School of Medicine, Indianapolis, Ind.

Presented in part at the 4th Annual Meeting of the Oxygen Society, San Francisco, Calif, November 20–24, 1997, and at Experimental Biology '98, San Francisco, Calif, April 18–22, 1998.

Correspondence to Aron B. Fisher, MD, Institute for Environmental Medicine, University of Pennsylvania School of Medicine, 1 John Morgan Building, 3620 Hamilton Walk, Philadelphia, PA 19104-6068. E-mail abf@mail.med.upenn.edu

© 1998 American Heart Association, Inc.

production by the lung. One purpose of the present study was to evaluate the sensitivity of ROS generation in the high- $K^+$  model to DPI and allopurinol. The results obtained indicate that the pattern of response with high  $K^+$  is similar to oxygenated ischemia and is different from anoxia/reoxygenation.

A second goal of the present study was to identify the DPI-sensitive metabolic pathway for ROS generation with oxygenated lung ischemia and with high  $K^+$ . Although DPI has been used as an inhibitor for the membrane-bound NADPH oxidase in phagocytes, such as polymorphonuclear leukocytes (PMNs),<sup>8</sup> its effect is not specific for this enzyme complex. Major components of the NADPH oxidase include the cytosolic proteins, p47<sup>phox</sup> and p67<sup>phox</sup>, and the membrane-bound flavocytochrome heterodimer comprising 2 polypeptides, p22<sup>phox</sup> and gp91<sup>phox</sup>.<sup>9,10</sup> The active enzyme complex is assembled at the plasma membrane in response to appropriate stimuli. Recently, the proline/arginine-rich 39-amino acid peptide PR-39 has been shown to inhibit the NADPH oxidase activity of PMNs by blocking oxidase assembly.<sup>11,12</sup> The availability of synthetic PR-39 allowed us to evaluate the role of NADPH oxidase assembly in lung ROS generation. As an additional approach, we evaluated ROS generation during oxygenated lung ischemia or high  $K^+$  in mice lacking ("knockout") gp91<sup>phox</sup>.<sup>13</sup> Through use of the inhibitory peptide and the knockout model, we show the primary role of the NADPH oxidase pathway for both lung ischemia and high- $K^+$  models of increased ROS generation.

## Materials and Methods

### Materials

PR-39, PR-26, and reverse PR-26 were synthesized from amino acids as previously described.<sup>12</sup> PR-26 is a truncated peptide (26 amino acids) that shows activity similar to PR-39; reverse PR-26 represents the same amino acid composition synthesized in the reverse direction as a control.<sup>12</sup> Allopurinol was purchased from Sigma Chemical Co. 2',7'-Dichlorodihydrofluorescein diacetate (H<sub>2</sub>DCF-DA) was obtained from Kodak; for use, a 5 mmol/L solution was prepared in absolute ethanol and stored under N<sub>2</sub> at -20°C in darkness. Acetylated LDL (AcLDL) tagged with fluorescent octadecyl indocarbocyanine (DiI-AcLDL) was obtained from Molecular Probes. DPI chloride was purchased from ICN Biochemicals. It should be noted that we have used the diphenyl rather than the diphenylene compound. JW-1, a polyclonal antibody raised against a C-terminal peptide of p47<sup>phox</sup> (residues 367 to 390, PRPSADLILNRCSESTKRKLASAC),<sup>14</sup> was a gift from Dr O.T.G. Jones (Bristol, UK). Nitrocellulose membrane was from Schleicher & Schuell. Horseradish peroxidase-conjugated goat anti-rabbit IgG and an enhanced chemiluminescence kit were purchased from Amersham. Molecular mass standards for SDS-PAGE and a protein dye-binding kit were from Bio-Rad Laboratories.

### Cell Culture

BPAECs were supplied as CCL-209 from the American Type Culture Collection. Cells were grown in MEM containing Earle's salts, 0.1 mmol/L nonessential amino acids, 15% FBS, 1 mmol/L sodium pyruvate, 1 mg/mL streptomycin, and 100 U/mL penicillin. Cells at passage 15 were seeded into 6-well plates (Falcon, Becton Dickinson & Co) at a density of  $4 \times 10^5$  cells/mL and maintained in a humidified atmosphere of 5% CO<sub>2</sub>/95% air.

For all experiments, plates of BPAECs at 1 to 2 days after confluence were washed 3 times with Krebs-Ringer bicarbonate (KRB) solution (mmol/L: NaCl 118.45, KCl 4.74 MgSO<sub>4</sub> · 7H<sub>2</sub>O 1.17, CaCl<sub>2</sub> · 2H<sub>2</sub>O 1.27, KH<sub>2</sub>PO<sub>4</sub> 1.18, and NaHCO<sub>3</sub> 24.87, pH 7.4,

supplemented with 10 mmol/L HEPES and 5.5 mmol/L glucose). Cells were loaded with dye by incubation with 5 μmol/L H<sub>2</sub>DCF-DA in KRB for 30 minutes. In some experiments, DPI, allopurinol, or a PR-39-related peptide was added during the 30-minute preincubation. After dye loading, cells were washed and incubated with dye-free KRB plus or minus inhibitors for 30 minutes at 37°C. Cells then were scraped, pelleted, washed with KRB, sonicated in 3 mL KRB, and recentrifuged (all carried out at 4°C). Fluorescence of the cell supernatant was measured as described below to assess ROS generation. In some experiments, 24 mmol/L KCl was substituted for equimolar NaCl in the KRB used for cell incubation.

### Isolated Lung Perfusion

The isolated perfused rat lung model used for the present study has been described previously.<sup>15</sup> Briefly, Sprague-Dawley male rats (Charles River Breeding Laboratories, Kingston, NY) weighing 180 to 200 g were anesthetized with intraperitoneal pentobarbital (30 mg/kg). Ventilation was maintained at 60 cycles/min, 2 mL tidal volume, and 2 cm H<sub>2</sub>O end-expiratory pressure. The chest was opened, and the pulmonary circulation was cleared of blood by gravity flow of perfusate with 25 cm H<sub>2</sub>O pressure through a cannula inserted in the main pulmonary artery, exiting from the transected left ventricle. The perfusate was KRB as described above (without HEPES) but modified by the addition of 3% (wt/vol) fatty acid-free BSA (Boehringer-Mannheim Biochemicals) or dextran (clinical grade, 70 to 90 kDa, Sigma) for fluorescence studies. High- $K^+$  (24 mmol/L) KRB was prepared as described above and substituted for KRB in some experiments. Perfusate was preequilibrated with the same gas mixture subsequently used for lung ventilation. The cleared lungs were freed of cardiac and other nonpulmonary tissues and were suspended in a water-jacketed perfusion chamber maintained at 37°C. Perfusion was maintained using a peristaltic pump at a constant flow rate of 10 mL/min with a recirculating volume of 40 mL. Lungs were ventilated with 95% O<sub>2</sub>/5% CO<sub>2</sub> for control, ischemia, and reoxygenation conditions and with 95% N<sub>2</sub>/5% CO<sub>2</sub> for anoxia (all gases were supplied by the BOC Group, Inc). Global ischemia was produced by discontinuing perfusion for 1 hour while ventilation continued. H<sub>2</sub>DCF-DA was added to the lung perfusate to make a final concentration of 5 μmol/L. Preperfusion with the fluorophore and inhibitors, if indicated, was for 30 minutes before the initiation of ischemia or high  $K^+$ . At the end of the perfusion experiment, the lungs were rapidly frozen by clamping with aluminum tongs precooled in liquid N<sub>2</sub>. The frozen lungs were homogenized and centrifuged; dichlorofluorescein (DCF) fluorescence of the supernatant was determined as described below. In additional experiments without H<sub>2</sub>DCF-DA, homogenization was carried out under N<sub>2</sub> in the presence of 0.01% butylated hydroxytoluene as previously described,<sup>1</sup> and the homogenate was assayed for thiobarbituric acid reactive substance (TBARS).

The generation of homozygous mice deficient in gp91<sup>phox</sup> (knockout) has been described previously.<sup>13</sup> The knockout mice used in the present study were derived from litters born after >10 generations of backcrosses into C57B16/J, the wild-type strain (Jackson Labs, Bar Harbor, Me). Mice weighing ≈25 g were anesthetized, and lungs were prepared for isolated lung perfusion. The protocol for mouse lung isolation and perfusion was similar to that used for rat lungs, but parameters were scaled down for the smaller size. Lungs were ventilated with 0.3 mL tidal volume at 60 cycles/min and perfused at 2 mL/min.

### Measurement of ROS Generation

Generation of ROS in BPAECs and in perfused lungs was monitored with H<sub>2</sub>DCF-DA fluorescence as previously described.<sup>16</sup> After internalization, the acetate group from the nonfluorescent molecule is cleaved by intracellular esterases with formation of H<sub>2</sub>DCF, which serves as a substrate for intracellular ROS to generate highly fluorescent DCF. Fluorescence was measured with a spectrofluorometer (model MPF-2A, Hitachi Perkin-Elmer) with 488-nm excitation and 530-nm emission. Data were expressed in arbitrary fluorescence units (AFU) relative to cell or lung protein measured with the Coomassie blue dye binding assay<sup>17</sup> using bovine gamma globulin as

the standard according to the directions of the supplier. TBARS were assayed in the lung homogenate by the method of Buege and Aust<sup>18</sup> and expressed as picomoles per milligram protein.

### Intravital Subpleural Microvascular Microscopy

We used an intravital microscopy technique to observe and image lung cells in situ in the isolated rat lung as described previously.<sup>5</sup> The ventilated and perfused rat lung was placed horizontally on a 48×60-mm coverglass window in a specially designed chamber. The chamber was placed on the stage of an epifluorescence microscope fitted with a ×100 objective (Nikon Diaphot TMD) and equipped with an optical filter changer (Lambda 10-2, Sutter Instrument Co).

Excitation of the lung surface was accomplished with a mercury lamp fiberoptic light source, narrow bandpass filters (FITC-485/10, Rhod-560/10), and a triple-band dichroic mirror (D/F/R-BS&M, Chroma Technology Corp). The emitted light passed through a narrow triple-bandpass filter (470/40, 535/40, and 630/60 peak transmission/half bandwidth, in nanometers). The objective was positioned so that the microvascular diameter was maximum at the focal plane. Images from the microscope were acquired during a 500-millisecond exposure time with a computer-controlled cooled CCD camera (MicroMAX, Princeton Instruments, Inc) using graphics control software (Metamorph Imaging System, Universal Imaging Corp). Ventilation was stopped briefly (<10 seconds) to permit collection of fluorescence images. Fluorescence images were acquired under control conditions for DCF and DiI-AcLDL in order to evaluate colocalization of the dyes. DiI-AcLDL is considered an endothelium-specific marker.<sup>19</sup> The DiI fluorescence signal was not observed in the DCF channel, whereas DCF contributed <10% of the DiI signal. Fluorescence images from the same area were taken sequentially using appropriate filter combinations for each dye and were overlaid for colocalization after assigning a separate pseudocolor to each image of a pair with the graphics software program. DCF fluorescence was evaluated for global lung ischemia, anoxia/reoxygenation, and perfusion with high K<sup>+</sup>.

### Western Blot of BPAEC Cytosolic Fraction

The cytosolic fraction from confluent BPAECs was isolated by differential centrifugation by modification of the method previously described for human fibroblasts.<sup>14</sup> Ten T-75 flasks with confluent BPAECs were cut open and washed 3 times with extraction buffer consisting of (mmol/L) Tris 50 (pH 7.5), EDTA 1, phenylmethylsulfonyl fluoride 1, and benzamidine 1. Cells were scraped with 300 mL extraction buffer, pooled, and sonicated on ice for three 20-second bursts at 50 W. The sonicate was centrifuged at 9000g for 10 minutes, and the resultant supernatant was centrifuged at 100 000g for 45 minutes (both at 4°C); the resulting supernatant was collected as the cytosolic fraction. Cytosolic proteins were precipitated with 10% trichloroacetic acid on ice, pelleted in a microfuge, washed twice with acetone, N<sub>2</sub>-dried, resuspended in SDS-PAGE sample buffer, and boiled for 2 minutes before electrophoresis. The proteins were separated by SDS-PAGE in a 10% separating gel, transferred to nitrocellulose paper by electroblotting, and probed with anti-p47<sup>phox</sup> polyclonal antibody, JW-1. Blots were developed using enhanced chemiluminescence.

### Immunocytochemistry and Histochemistry With Anti-p47<sup>phox</sup> Antibody

Rat and mouse lungs were cleared of blood. Tissue pieces were fixed with 4% paraformaldehyde for 3 hours, washed, treated sequentially with 10%, 20%, and 30% sucrose overnight, frozen in liquid N<sub>2</sub> and methyl butane, and kept at -80°C until sectioned. BPAECs were seeded on 8-well tissue culture slides at a density of 2.5×10<sup>4</sup> cells per well, allowed to adhere overnight, and fixed for 15 minutes in 4% paraformaldehyde. Slides with fixed tissue sections or cells were washed twice alternately with PBS (50 mmol/L Na<sub>2</sub>HPO<sub>4</sub> and 136 mmol/L NaCl, pH 7.2) containing 0.3% Triton X-100 or 0.1% NaBH<sub>4</sub>. Nonspecific antibody binding sites were blocked by 30 minutes of incubation in PBS containing 0.3% Triton X-100, 5% BSA, and 10% normal goat serum. The slides were washed with PBS

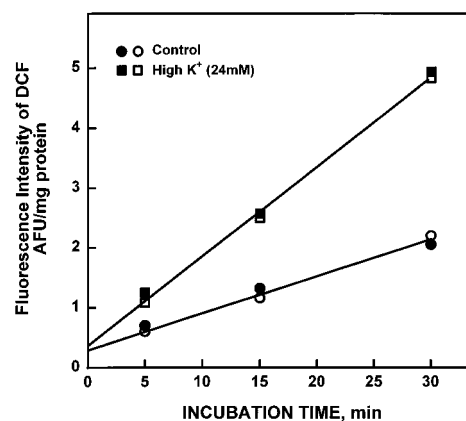


**Figure 1.** Time course of ROS generation in BPAECs. BPAECs were prelabeled with H<sub>2</sub>DCF-DA for 30 minutes, the dye was removed, and cells were incubated with control (5 mmol/L K<sup>+</sup>) or iso-osmotic high-K<sup>+</sup> (24 mmol/L) medium for the indicated time. Data are from separate experiments indicated by open (experiment 1) and closed (experiment 2) symbols.

containing 0.3% Triton X-100 for 5 minutes, incubated for 3 hours in a moist chamber at room temperature with JW-1 (1:1000 dilution) or nonimmune rabbit IgG, washed again with PBS+0.3% Triton X-100, and incubated for 1 hour with Texas Red-conjugated secondary goat anti-rabbit antibody. The slides were washed twice with PBS+0.3% Triton X-100 for 5 minutes each, air-dried, and coverslipped with Mowiol (Calbiochem). Epifluorescence digital micrographs were taken at 545-nm excitation and 585-nm emission with the use of a Nikon Diaphot microscope and MicroMax CCD camera (Princeton Instruments) run by Metamorph Image Acquisition software (Universal Imaging Corp).

### Statistics

Incubations for BPAECs generally were carried out in duplicate, and the individual results were averaged; perfused lung data represent the mean±SE of individual experiments unless otherwise indicated. Statistical analysis was carried out by ANOVA using Sigma Stat (Jandel). The level of statistical significance was taken as *P*<0.05.

### Results

BPAECs under resting conditions generated ROS, as indicated by oxidation of H<sub>2</sub>DCF at a rate that was approximately linear for 30 minutes of incubation (Figure 1). Allopurinol (100 μmol/L) or PR-39 (10 μmol/L) had no effect on ROS generation by control cells, whereas DPI (100 μmol/L) significantly inhibited ROS production by ≈50% (Table 1). The effect of DPI suggests that basal ROS production occurs through NADPH oxidase or a related flavoprotein. The failure of PR-39 to inhibit basal activity is consistent with its postulated role in preventing assembly of the enzyme com-

**TABLE 1.** Effect of Inhibitors on H<sub>2</sub>DCF Oxidation by Resting BPAECs

	AFU, 30 min/mg Protein	% of Control
Control	3.76±0.071	100
+Allopurinol, 100 μmol/L	3.81±0.058	101
+DPI, 100 μmol/L	1.67±0.018*	44
+PR-39, 10 μmol/L	3.81±0.24	101
+PR-26, 10 μmol/L	3.66±0.15	97

Values are mean±SE AFU (n=10 for control and n=3 for inhibitors).

\**P*<0.05 vs control.



**TABLE 2. Effect of Inhibitors on High K<sup>+</sup>-Induced ROS Generation by BPAECs**

	ΔAFU, 30 min/mg Protein	% Inhibition
High K <sup>+</sup> (control)	3.30±0.20	...
+Allopurinol, 100 μmol/L	3.12±0.19	5
+DPI, 100 μmol/L	0.66±0.055*	80

Cells were incubated with 24 mmol/L K<sup>+</sup>. The increase in AFU (ΔAFU) was calculated as total AFU minus AFU with the corresponding inhibitor during incubation of resting cells in 5 mmol/L K<sup>+</sup> (Table 1). Values are mean±SE (n=10 for high K<sup>+</sup> and n=3 for inhibitors).

\*P<0.05 vs high K<sup>+</sup> (control).

plex,<sup>12</sup> in contrast to DPI, which prevents flux through already assembled enzyme.<sup>8</sup> Cells after DPI treatment showed no change in viability, as determined by exclusion of erythrocin B dye (data not shown).

The rate of H<sub>2</sub>DCF oxidation by BPAECs during 30 minutes increased ≈2.5-fold in the presence of high (24 mmol/L) K<sup>+</sup> (Figure 1). This result with an intracellular fluorescence probe is consistent with our previous data obtained by assay of oxidants released into the incubation medium.<sup>7</sup> High K<sup>+</sup>-induced ROS generation by the cells was essentially abolished by DPI, whereas allopurinol had no effect (Table 2). PR-39 also inhibited K<sup>+</sup>-induced ROS generation by BPAECs (Figure 2). The effect of PR-39 was concentration dependent, with an estimated 50% inhibition at ≈3 μmol/L. The truncated peptide, PR-26, was equivalent to PR-39 as an inhibitor. Reverse PR-26, used as a control for nonspecific effects of the peptide, had no effect on ROS generation.

We next studied the effect of inhibitors on high K<sup>+</sup>-induced ROS generation by the isolated perfused rat lung. The basal level of DCF fluorescence detected in the homogenate of the perfused lung at the end of the equilibration period increased only slightly during 1 hour of perfusion under control conditions (Figure 3). In the presence of high

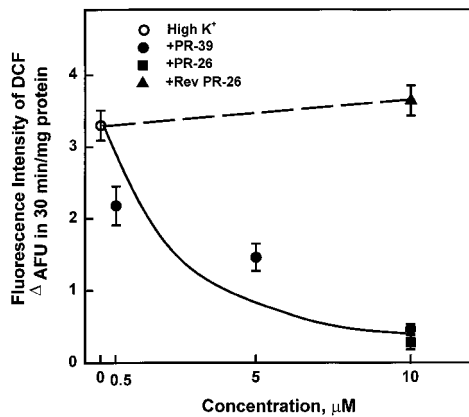


**Figure 2.** Effect of PR-39 on high K<sup>+</sup>-induced ROS generation in BPAECs. Cells were preincubated with H<sub>2</sub>DCF-DA for 30 minutes. After removal of dye, medium was changed to 24 mmol/L K<sup>+</sup> for an additional 30-minute incubation. PR-39 in varying concentrations or related peptides were added during both the preincubation and incubation periods. Rev PR-26 indicates reverse PR-26. DCF fluorescence represents the increase above the value for resting cells as described in Table 2. Each point represents the mean±SE for 3 separate experiments.

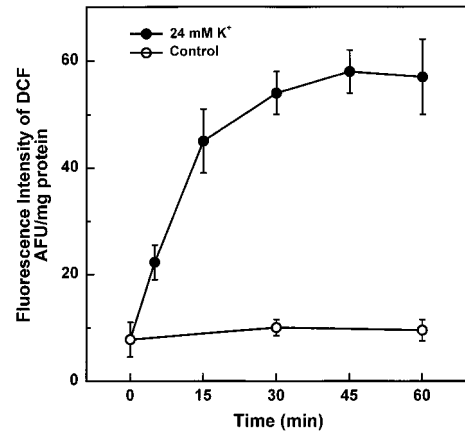


**Figure 3.** Effect of perfusate high K<sup>+</sup> on ROS generation in isolated rat lungs. Isolated blood-free rat lungs were preperfused with buffer containing 5 μmol/L H<sub>2</sub>DCF-DA for 30 minutes. Lungs then were perfused for varying times, after which DCF fluorescence was determined in the lung homogenate. Control perfusate contained 5 mmol/L K<sup>+</sup>; high-K<sup>+</sup> perfusate was 24 mmol/L under iso-osmotic conditions. Data are mean±range for 2 lungs for each condition.

K<sup>+</sup>, ROS generation increased significantly during the initial 15 minutes of perfusion and reached a plateau level at ≈30 minutes (Figure 3). The increase at the plateau was ≈6-fold over the control value. ROS generation was not significantly changed in the presence of allopurinol but was essentially abolished in the presence of either DPI or PR-39 (Figure 4).

We have previously shown that DPI markedly inhibits ROS generation associated with lung ischemia, whereas allopurinol has no effect.<sup>3</sup> In the present study, the effect of PR-39 on ROS generation with ischemia was evaluated. Ischemia for 60 minutes resulted in a 7-fold increase in DCF fluorescence (Figure 5), similar to that previously reported from our laboratory.<sup>3</sup> Preperfusion with PR-39 resulted in a concentration-dependent inhibition of ROS generation (Fig-

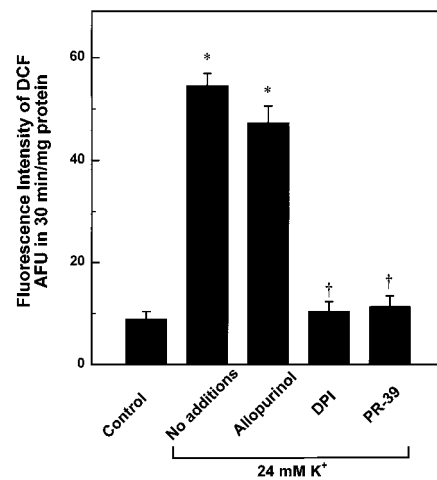


**Figure 4.** Effect of inhibitors on high K<sup>+</sup>-induced ROS generation in perfused rat lungs. After loading with H<sub>2</sub>DCF as described in Figure 3, lungs were perfused with 5 mmol/L K<sup>+</sup> (control) or 24 mmol/L K<sup>+</sup> for 30 minutes, and DCF fluorescence in the lung homogenate was measured. Inhibitors were 100 μmol/L allopurinol, 100 μmol/L DPI, or 10 μmol/L PR-39. Data are mean±SE for n=4 for each condition. \*P<0.05 vs control; †P<0.05 vs high K<sup>+</sup> (no additions).

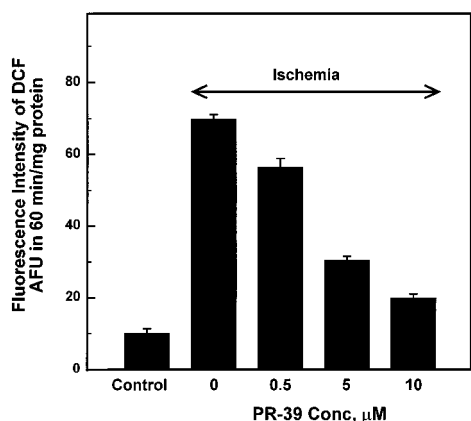


**Figure 5.** Effect of varying concentrations of PR-39 (PR-39 Conc) on ischemia-induced ROS generation in continuously ventilated rat lungs. DCF fluorescence was measured in homogenates from control lungs perfused continuously for 1 hour or in lungs after 1 hour of global ischemia. Data are mean  $\pm$  SE ( $n=3$  for each condition).

ure 5). PR-39 at 10  $\mu\text{mol/L}$  inhibited ROS generation by 80%, and the concentration for 50% inhibition was  $\approx 3 \mu\text{mol/L}$ , similar to that observed for  $\text{K}^+$ -induced ROS generation with cultured BPAECs.

The effect of PR-39 is consistent with a role for NADPH oxidase in the production of ROS associated with high  $\text{K}^+$  or ischemia. We next investigated mice with a knockout of gp91<sup>phox</sup>, a cytochrome component of this oxidase. Similar to the findings with rat lungs, isolated ventilated lungs from wild-type mice showed a large increase (7-fold) in DCF fluorescence after exposure to high  $\text{K}^+$  or ischemia, indicating ROS production (Figure 6). In contrast to the wild-type mice, there was no significant change in DCF fluorescence in response to high  $\text{K}^+$  or ischemia in the knockout mice, indicating that gp91<sup>phox</sup> is required for ROS production in these models (Figure 6). Anoxia/reoxygenation in lungs from these mice resulted in a 4-fold increase in DCF fluorescence, and there was no difference between control and knockout

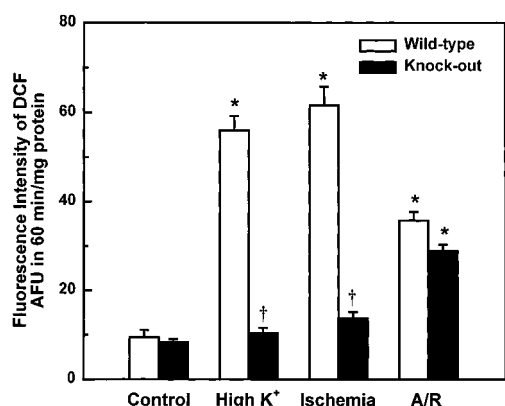


**Figure 6.** ROS generation during high  $\text{K}^+$  perfusion, ischemia, or anoxia/reoxygenation (A/R) in isolated lungs from wild-type and gp91<sup>phox</sup> knockout mice. Continuously ventilated mouse lungs were perfused with 24 mmol/L  $\text{K}^+$  or were subjected to 1 hour of global ischemia or to 1 hour of anoxia produced by ventilation with 95%  $\text{N}_2/5\% \text{CO}_2$  followed by 1 hour of reoxygenation. Data are mean  $\pm$  SE for 4 lungs for each condition. \* $P < 0.05$  vs corresponding control; † $P < 0.05$  vs corresponding wild type.

lungs (Figure 6). This result is compatible with findings that indicated different pathways for the generation of ROS in rat lungs exposed to ischemia and anoxia/reoxygenation.<sup>3</sup>

To localize the cells responsible for ROS generation with lung ischemia, we used an in situ fluorescence imaging technique. We used DiI-AcLDL as an endothelial marker and  $\text{H}_2\text{DCF-DA}$  to image ROS generation. These dyes showed strong colocalization in the rat lung, indicating that endothelial cells were the primary site of  $\text{H}_2\text{DCF}$  localization and were responsible for the major fraction of DCF fluorescence (Figure 7). Lung ischemia led to a marked increase in alveolar capillary-associated DCF fluorescence, confirming endothelium as a major source of ROS generation (Figure 8). High  $\text{K}^+$  and anoxia/reoxygenation also led to increased fluorescence that was predominantly localized to the endothelial compartment (Figure 8). Essentially no PMNs were observed, and macrophages were rare in these lungs, so that phagocytes made no significant contribution to the fluorescence signals.

The above results indicate that PR-39 inhibits both  $\text{K}^+$ -induced and ischemia-induced ROS generation in lung models. PR-39 also prevented oxidative lung injury, as indicated by lipid peroxidation products. Both ischemia-induced and high  $\text{K}^+$ -induced TBARS production was inhibited significantly by pretreatment of perfused rat lungs with 10  $\mu\text{mol/L}$  PR-39 (Figure 9).

In PMNs, PR-39 inhibits ROS production by blocking the interaction of cytoplasmic p47<sup>phox</sup> with the membrane-localized cytochrome subunit, p22<sup>phox</sup>.<sup>12</sup> Therefore, we evaluated BPAECs and rat lungs for the possible presence of this key component of the membrane NADPH oxidase. Western blot using anti-p47<sup>phox</sup> antibody with the soluble fraction from BPAECs showed an immunoreactive band at  $\approx 47 \text{ kDa}$  (Figure 10). Immunocytochemistry of cultured BPAECs demonstrated a strong reaction to p47<sup>phox</sup> antibody, whereas control IgG was negative (Figure 11). Immunohistochemistry of rat lungs indicated strong reaction in the vascular endothelium and in the alveolar septae compatible with endothelial localization of p47<sup>phox</sup> (Figure 11).

## Discussion

The present study has used both cultured cells and isolated perfused rat and mouse lungs to investigate pathways for ROS generation associated with lung ischemia and with a high- $\text{K}^+$  model for membrane depolarization. We confirmed our previous studies that showed increased ROS generation in response to high  $\text{K}^+$  in both BPAECs<sup>6</sup> and perfused lungs<sup>7</sup> and in response to oxygenated ischemia in the isolated rat lung,<sup>2</sup> and we demonstrated similar results in the mouse lung. The indicator for ROS generation was the oxidation of  $\text{H}_2\text{DCF}$  to the fluorescent DCF. This fluorophore, which has been used widely in studies of ROS generation in PMNs and other cells,<sup>20-22</sup> was used in previous studies of lung ischemia and anoxia/reoxygenation.<sup>3,17</sup> Although  $\text{H}_2\text{DCF}$  has been used to detect  $\text{H}_2\text{O}_2$  in vitro, it is sensitive to other radical species and cannot be considered specific when used in cells or organs.<sup>23</sup> For that reason, we have used the generic term ROS for the products detected.

On the basis of the fluorescence imaging studies in the isolated rat lung, endothelium was the major site for increased

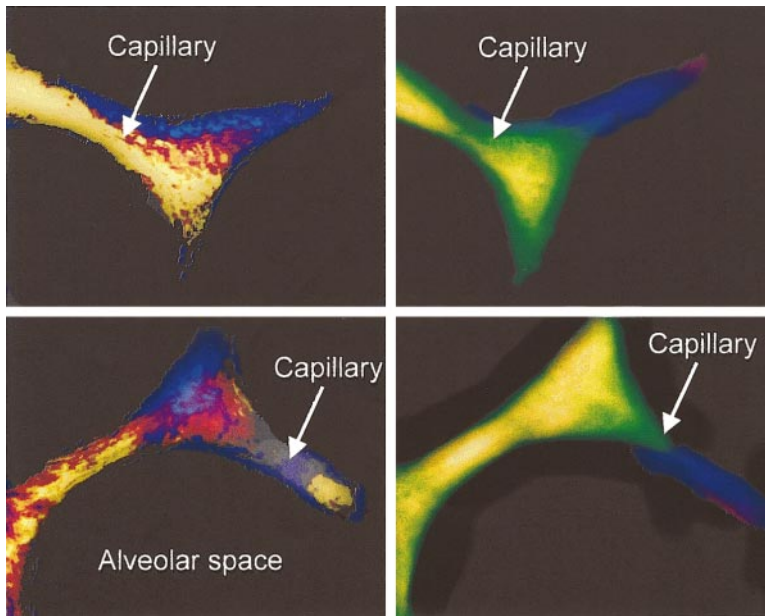


**Figure 7.** In situ imaging of lungs to evaluate colocalization of DCF and the endothelial marker Dil-AcLDL. Isolated rat lungs were perfused with 30  $\mu$ g Dil-AcLDL and 5  $\mu$ mol/L H<sub>2</sub>DCF-DA for 30 minutes and then placed on a microscope stage for in situ imaging of subpleural endothelium as described in Materials and Methods. Images from the same area were taken at excitation/emission of 545/585 nm for Dil-AcLDL (left panels) and 490/530 for DCF (right panels). The DCF and Dil-AcLDL labels, shown pseudocolor, are largely colocalized. Horizontal dimension of each panel is 87  $\mu$ m.

oxidation of the fluorophore, H<sub>2</sub>DCF, in all 3 models: lung ischemia, high K<sup>+</sup>, and anoxia/reoxygenation. This localization presumably reflects the potential of these cells for ROS production but also may reflect in part the relatively greater

accessibility of capillary endothelial cells to the fluorophore delivered via the perfusate. More generalized labeling of lung cells in our previous study<sup>16</sup> was seen with prolonged perfusion (1 to 2 hours) with H<sub>2</sub>DCF-DA and was confirmed in the present study by imaging with carboxyfluorescein diacetate (data not shown). To evaluate the role of endothelium, lungs were perfused with synthetic medium to eliminate the effects of blood elements and to minimize a potential contribution from intravascular cells such as PMNs. In situ imaging of lungs did not show fluorescence arising from phagocytes. These observations coupled with the relatively high percentage ( $\approx$ 33%) of capillary endothelial cells to total lung cells lead to the conclusion that the response of lung DCF fluorescence to metabolic inhibitors in our model reflects primarily ROS generation by pulmonary capillary endothelium.

ROS production with ischemia in the isolated lung was unaffected by the presence of allopurinol but was significantly inhibited with DPI.<sup>3</sup> By contrast, the inverse result was

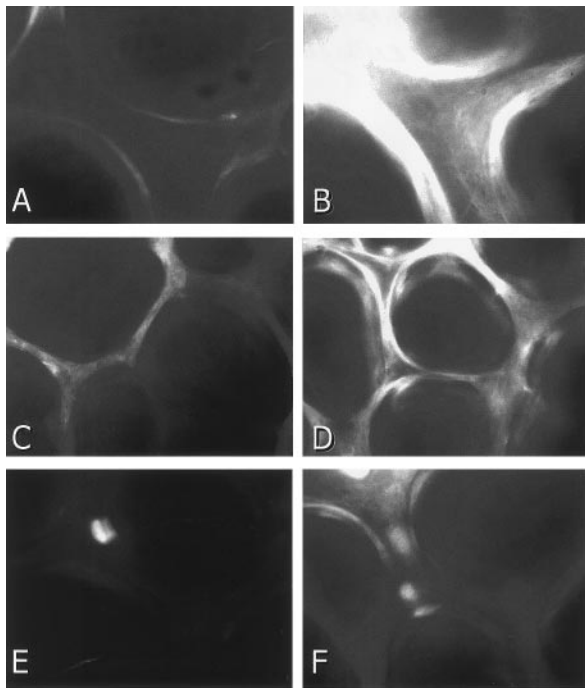


**Figure 8.** Localization of increased DCF fluorescence in response to ischemia, high K<sup>+</sup>, and anoxia/reoxygenation by in situ imaging. Isolated ventilated rat lungs were perfused with 5  $\mu$ mol/L H<sub>2</sub>DCF-DA for 30 minutes. Images were taken at excitation/emission of 490/530 nm during control perfusions (left panels) and time-matched experimental perfusions (right panels). The darker areas represent the nonfluorescent alveolar space. The increase in DCF fluorescence with each of the experimental conditions indicates ROS generation by the endothelium in situ. Horizontal dimension is 87  $\mu$ m for panels A and B and 148  $\mu$ m for panels C to F. A, Control perfusion, 1 hour. B, Ischemia, 1 hour. C, Control perfusion, 30 minutes. D, Perfusion with 24 mmol/L K<sup>+</sup>, 30 minutes. E, Control perfusion, 90 minutes. F, Anoxia, 1 hour followed by reoxygenation, 30 minutes.

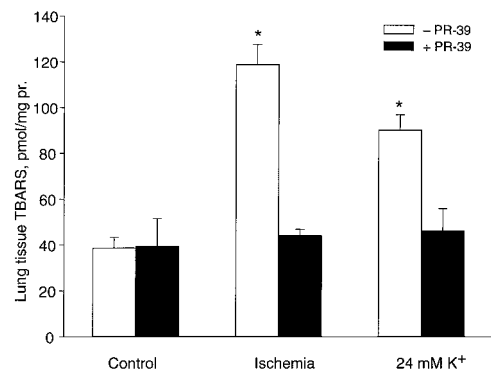


**Figure 9.** Effect of PR-39 on ischemia-induced or high K<sup>+</sup>-induced lipid peroxidation. Lungs were subjected to 1 hour of ischemia or perfused with 24 mmol/L K<sup>+</sup> with or without 10  $\mu$ mol/L PR-39 pretreatment for 30 minutes. TBARS was measured in the lung homogenate as described in Materials and Methods. Values are mean  $\pm$  SE (n=4). \*P<0.05 vs control or corresponding conditions without PR-39.



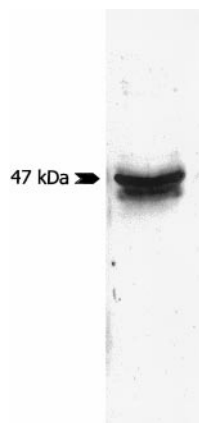


**Figure 10.** Western blot analysis of BPAEC cytosolic fraction proteins for p47<sup>phox</sup>. Proteins were separated by SDS-PAGE, transferred to nitrocellulose membrane, and probed with JW-1, a polyclonal anti-p47<sup>phox</sup> antibody. Blots were developed using enhanced chemiluminescence.

obtained with lung anoxia/reoxygenation.<sup>3</sup> Therefore, xanthine oxidase is the apparent source of ROS with anoxia/reoxygenation, whereas ROS generation with lung ischemia appears to be mediated through a different flavoprotein. The spectrum of inhibition for high K<sup>+</sup> perfusion was similar to that for ischemia; ie, allopurinol had no effect, whereas DPI resulted in marked inhibition of ROS generation. PR-39–

mediated inhibition of DCF fluorescence in response to both high K<sup>+</sup> and lung ischemia suggests that NADPH oxidase is the flavin-linked enzyme source of ROS. The gp91<sup>phox</sup> knockout mouse model confirmed the role of NADPH oxidase in ROS production with lung ischemia and high-K<sup>+</sup> models.

The membrane-bound NADPH oxidase of PMN and other phagocytic cells represents a complex of at least 2 cytosolic and 2 intrinsic membrane proteins.<sup>9,10</sup> A requirement for assembly of this complex is the binding of cytoplasmic p47<sup>phox</sup> to the membrane components.<sup>10,12</sup> The presence of several components of this oxidase system has been demonstrated previously in endothelial cells derived from human umbilical veins.<sup>24</sup> The present study using a polyclonal antibody demonstrates the presence of p47<sup>phox</sup> in BPAECs and in rat lung endothelium, thus providing a basis for the effect of PR-39. PR-39 inhibited ROS generation compatible with the demonstrated effect of this agent, which binds to Src homology 3 domains of p47<sup>phox</sup>, thereby preventing its assembly with p22<sup>phox</sup>.<sup>12</sup> Results with the knockout mouse model provide evidence for the presence of gp91<sup>phox</sup>, one of the intrinsic membrane proteins required for NADPH oxidase activity. Thus, the components of this pathway as described for PMNs appear to be present in pulmonary endothelium. Although other lung cell types have been shown previously to express this enzyme,<sup>25,26</sup> this is the first demonstration of the presence of the enzyme in lung endothelial cells.

In previous studies, production of ROS by cultured bovine pulmonary endothelial cells was demonstrated in response to reoxygenation after prolonged (12 to 24 hours) hypoxia.<sup>27</sup> The generation of ROS in this lung-cell model was sensitive in part to DPI and also in part to allopurinol,<sup>28,29</sup> confirming that these cells can produce ROS through at least 2 separate pathways. Localization of the DPI-sensitive pathway to the cell membrane and its inhibition by DPI suggest a role for NADPH oxidase.<sup>28</sup> On the other hand, knockout of gp91<sup>phox</sup> (present study) or the presence of DPI<sup>3</sup> had no effect on ROS with anoxia/reoxygenation in the intact isolated lung. The reason for the different response to prolonged hypoxia in cultured cells and to acute anoxia in the perfused lung is not clear. Clearly, the acute models of ischemia and anoxia/reoxygenation in the lung activate separate ROS-generating pathways, whereas both pathways appear to be activated with prolonged hypoxia/reoxygenation in the cultured cells.

We have shown previously that high external K<sup>+</sup> leads to ROS generation by lungs and BPAECs and have suggested this as a model for ischemia-mediated oxidant generation.<sup>6,7</sup> The present study provides additional evidence that high K<sup>+</sup> and lung ischemia lead to ROS generation through a common mechanism. The proposed common mechanism for these 2 models is ROS generation associated with endothelial cell membrane depolarization. A similar association between membrane depolarization and ROS generation via the respiratory burst has been demonstrated for PMN and other phagocytic cells.<sup>30–32</sup> We have postulated that ischemia with the attendant absence of flow leads to membrane depolarization in pulmonary endothelium,<sup>5</sup> possibly through inactivation of shear stress-sensitive K<sup>+</sup> channels.<sup>33</sup> In support of this hypothesis, we have demonstrated membrane depolarization with ischemia in the isolated rat lung through the use of

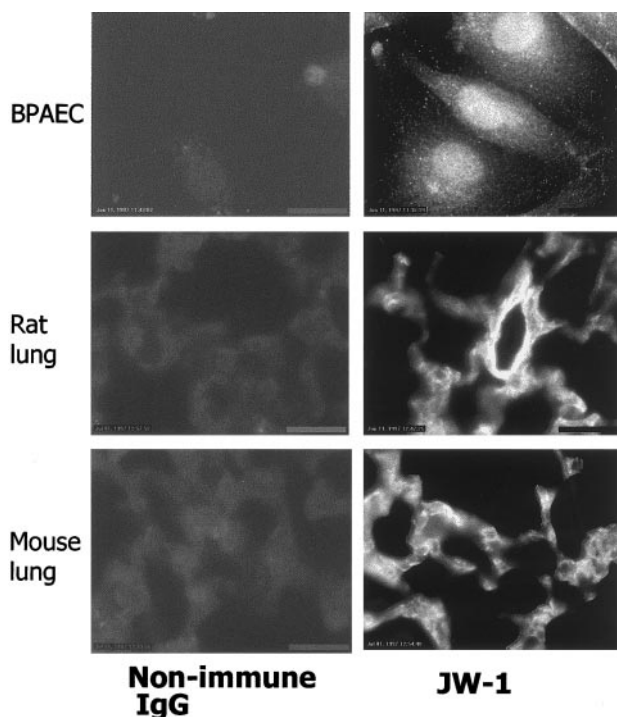


**Figure 11.** Immunocytochemistry of BPAEC, rat lung, and mouse lung for p47<sup>phox</sup>. Fixed BPAECs and lung sections were treated with rabbit nonimmune IgG (left column) or JW-1 antibody (right column). Goat anti-rabbit IgG conjugated with Texas Red served as the secondary antibody. Epifluorescence micrographs were taken at 545-nm excitation and 585-nm emission. Increased fluorescence in JW-1 antibody-treated sections indicates the presence of p47<sup>phox</sup> in BPAECs and in rat and mouse lung endothelium. The vertical dimension is 34  $\mu$ m for BPAEC panels and 68  $\mu$ m for lung section panels.

membrane potential-sensitive fluorophores,<sup>5</sup> although the responsible channels have not yet been identified. The present results demonstrate that the pathway for ROS production with ischemia is a membrane-associated NADPH oxidase of pulmonary endothelium and suggest that membrane depolarization with ischemia initiates the assembly and activation of this enzyme complex.

We have demonstrated previously that ROS production during lung ischemia or in response to high K<sup>+</sup> results in oxidation of tissue components as indicated by measurement of tissue TBARS and protein carbonyls.<sup>1-3,7,34,35</sup> Lipid peroxidation with ischemia is markedly inhibited by the presence of DPI.<sup>3</sup> In the present study, we have shown that PR-39 also inhibits the lipid peroxidation resulting from ischemia as well as high-K<sup>+</sup> perfusion. Thus, inhibition of the NADPH oxidase pathway protects lung tissue against ROS-mediated injury.

### Acknowledgments

This study was supported by NIH grants HL-41939 and HL-52565 (Dr Fisher) and a Parker B. Francis Fellowship (Dr Al-Mehdi). We thank Drs Owen Jones and Simon Jones for providing the antibody to p47<sup>phox</sup>, Dr Claire Doerschuk for suggesting the use of the knockout mice, Dr Jahar Bhattacharya for advice concerning lung imaging, June Nelson and Kathy Notarfrancesco for excellent technical assistance, and Elaine Primerano for typing the manuscript.

### References

- Fisher AB, Dodia C, Tan Z, Ayene I, Eckenhoof RG. Oxygen-dependent lipid peroxidation during lung ischemia. *J Clin Invest.* 1991;88:674-679.
- Al-Mehdi A, Shuman H, Fisher AB. Intracellular generation of reactive oxygen species during non-hypoxic lung ischemia. *Am J Physiol.* 1997;270:L294-L300.
- Zhao G, Al-Mehdi A, Fisher AB. Anoxia-reoxygenation versus ischemia in isolated rat lungs. *Am J Physiol.* 1997;273:L1112-L1117.
- McCord JM. Oxygen-derived free radicals in post-ischemic tissue injury. *N Engl J Med.* 1985;312:159-163.
- Al-Mehdi A, Zhao G, Fisher AB. ATP-independent membrane depolarization with ischemia in the oxygen-ventilated isolated rat lung. *Am J Respir Cell Mol Biol.* 1998;18:653-661.
- Al-Mehdi A, Ischiropoulos H, Fisher AB. Endothelial cell oxidant generation during K<sup>+</sup>-induced membrane depolarization. *J Cell Physiol.* 1996;166:274-280.
- Al-Mehdi A, Shuman H, Fisher AB. Oxidant generation with K<sup>+</sup>-induced depolarization in the isolated perfused lung. *Free Radic Biol Med.* 1997;23:47-56.
- Cross AR, Jones OT. The effect of the inhibitor diphenylene iodonium on the superoxide-generating system of neutrophils: specific labelling of a component polypeptide of the oxidase. *Biochem J.* 1986;237:111-116.
- Clark RA. The human respiratory burst oxidase. *J Infect Dis.* 1990;161:1140-1147.
- DeLeo FR, Quinn MT. Assembly of the phagocyte NADH oxidase: molecular interaction of oxidase proteins. *J Leukoc Biol.* 1996;60:677-691.
- Shi J, Ross CR, Chengappa MM, Blecha F. Identification of a proline-arginine-rich antibacterial peptide from neutrophils that is analogous to PR-39, an antibacterial peptide from the small intestine. *J Leukoc Biol.* 1994;56:807-811.
- Shi J, Ross CR, Leto TL, Blecha F. PR-39, a proline-rich antibacterial peptide that inhibits phagocyte NADPH oxidase activity by binding to Src homology 3 domains of p47<sup>phox</sup>. *Proc Natl Acad Sci U S A.* 1996;93:6014-6018.
- Pollock JD, Williams DA, Gifford MA, Li LL, Du X, Fisherman J, Orkin SH, Doerschuk CM, Dinauer MC. Mouse model of X-linked chronic granulomatous disease, an inherited defect in phagocyte superoxide production. *Nat Genet.* 1995;9:202-209.
- Jones SA, Wood JD, Coffey MF, Jones OTG. The functional expression of p47<sup>phox</sup> and p64<sup>phox</sup> may contribute to the generation of superoxide by an NADPH oxidase-like system in human fibroblasts. *FEBS Lett.* 1994;355:178-182.
- Fisher AB, Dodia C, Linask J. Perfusate composition and edema formation in isolated rat lungs. *Exp Lung Res.* 1980;1:13-21.
- Al-Mehdi A, Shuman H, Fisher AB. Fluorescence microtopography of oxidative stress in lung ischemia-reperfusion. *Lab Invest.* 1994;70:579-587.
- Bradford MM. A rapid and sensitive method for quantitation of microgram quantities of protein utilizing the principle of protein dye binding. *Anal Biochem.* 1976;72:248-254.
- Buege JA, Aust SD. Microsomal lipid peroxidation. *Methods Enzymol.* 1978;52:302-310.
- Voyta JC, Via DP, Butterfield CE, Zetter BR. Identification and isolation of endothelial cells based on their increased uptake of acetylated-low density lipoprotein. *J Cell Biol.* 1984;99:2034-2040.
- Trinkle LS, Welhausen SR, McLeish KR. A simultaneous flow cytometric measurement of neutrophil phagocytosis and oxidative burst in whole blood. *Diagn Clin Immunol.* 1987;5:62-68.
- Kobzik L, Godleski JJ, Brain JD. Oxidative metabolism in the alveolar macrophage: analysis by flow cytometry. *J Leukoc Biol.* 1990;47:295-303.
- Robertson FM, Beavis AJ, Oberszyn TM, O'Connell SM, Dokidos A, Laskin DL, Laskin JD, Reiners JJ Jr. Production of hydrogen peroxide by murine epidermal keratinocytes following treatment with the tumor promoter 12-O-tetradecanoylphorbol-13-acetate. *Cancer Res.* 1990;50:6062-6067.
- Crow JP. Dichlorodihydrofluorescein and dihydrorhodamine 123 are sensitive indicators of peroxynitrite *in vitro*: implications for intracellular measurement of reactive nitrogen and oxygen species. *Biol Chem.* 1997;1:145-157.
- Jones SA, O'Donnell VB, Wood JD, Broughton JP, Hughes EJ, Jones OTG. Expression of phagocyte NADPH oxidase components in human endothelial cells. *Am J Physiol.* 1996;271:H1626-H1634.
- Marshall C, Mamary AJ, Verhoeven AJ, Marshall BE. Pulmonary artery NADPH-oxidase is activated in hypoxic pulmonary vasoconstriction. *Am J Respir Cell Mol Biol.* 1996;15:633-644.
- Wang D, Youngson C, Wong V, Yeger H, Dinauer MC, Vega-Saenz Miera E, Rudy B, Cutz E. NADPH-oxidase and a hydrogen peroxide-sensitive K<sup>+</sup> channel may function as an oxygen sensor complex in airway chemoreceptors and small cell lung carcinoma cell lines. *Proc Natl Acad Sci U S A.* 1996;93:13182-13187.
- Lum H, Barr DA, Shaffer JR, Gordon RJ, Ezrin AM, Malik AB. Reoxygenation of endothelial cells increases permeability by oxidant-dependent mechanisms. *Circ Res.* 1992;70:991-998.
- Zulueta JJ, Yu FS, Hertig IA, Thannickal VJ, Hassoun PM. Release of hydrogen peroxide in response to hypoxia-reoxygenation: role of an NAD(P)H oxidase-like enzyme in endothelial cell plasma membrane. *Am J Respir Cell Mol Biol.* 1995;12:41-49.
- Zulueta JJ, Sawhney R, Yu FS, Cote CC, Hassoun PM. Intracellular generation of reactive oxygen species in endothelial cells exposed to anoxia-reoxygenation. *Am J Physiol.* 1997;272:L897-L902.
- Kuroki M, Kamo N, Kobatake Y, Okimassu E, Utsumi K. Measurement of membrane potential in polymorphonuclear leukocytes and its changes during surface stimulation. *Biochim Biophys Acta.* 1982;693:326-334.
- Kitagawa S, Johnston RB. Relationship between membrane potential changes and superoxide releasing capacity in resident and activated mouse peritoneal macrophages. *J Immunol.* 1985;35:3417-3423.
- Henderson LM, Chappell JB, Jones OT. Superoxide generation by the electrogenic NADPH-oxidase of human neutrophils is limited by the movement of a compensating charge. *Biochem J.* 1988;255:285-290.
- Olesen S, Clapham DE, Davies PF. Haemodynamic shear stress activates a K<sup>+</sup> current in vascular endothelial cells. *Nature.* 1988;331:168-170.
- Ayene SI, Dodia C, Fisher AB. Role of oxygen in oxidation of lipid and protein during ischemia/reperfusion in isolated perfused rat lung. *Arch Biochem Biophys.* 1992;296:183-189.
- Zhao G, Ayene IS, Fisher AB. Role of iron in ischemia-reperfusion oxidative injury of rat lungs. *Am J Respir Cell Mol Biol.* 1997;16:293-299.



# Circulation Research

JOURNAL OF THE AMERICAN HEART ASSOCIATION



## Endothelial NADPH Oxidase as the Source of Oxidants in Lungs Exposed to Ischemia or High $K^+$

Abu B. Al-Mehdi, Guochang Zhao, Chandra Dodia, Kasumi Tozawa, Karen Costa, Vladimir Muzykantov, Chris Ross, Frank Blecha, Mary Dinauer and Aron B. Fisher

*Circ Res.* 1998;83:730-737

doi: 10.1161/01.RES.83.7.730

*Circulation Research* is published by the American Heart Association, 7272 Greenville Avenue, Dallas, TX 75231

Copyright © 1998 American Heart Association, Inc. All rights reserved.

Print ISSN: 0009-7330. Online ISSN: 1524-4571

The online version of this article, along with updated information and services, is located on the World Wide Web at:

<http://circres.ahajournals.org/content/83/7/730>

**Permissions:** Requests for permissions to reproduce figures, tables, or portions of articles originally published in *Circulation Research* can be obtained via RightsLink, a service of the Copyright Clearance Center, not the Editorial Office. Once the online version of the published article for which permission is being requested is located, click Request Permissions in the middle column of the Web page under Services. Further information about this process is available in the [Permissions and Rights Question and Answer](#) document.

**Reprints:** Information about reprints can be found online at:  
<http://www.lww.com/reprints>

**Subscriptions:** Information about subscribing to *Circulation Research* is online at:  
<http://circres.ahajournals.org/subscriptions/>